J. Surface Sci. Technol., Vol 29, No. 3-4, pp. 1-11, 2013

Microstructural and Corrosion Resistance Studies on SUS 420F and EN32B Steels Under Surface Treatment by High Power Diode Laser

N. SIVANANDHAM[a], A. RAJADURAI[b], S. M. SHARIFF[c], J. SENTHILSELVAN[d] and A. MAHALINGAM[a] *

[a]*Department of Physics, Anna University, Chennai-600 025, India*
[b]*Department of Production Technology, MIT Campus, Anna University, Chennai-600 044, India*
[c]*International Advanced Research Centre for Powder Metallurgy and New Materials (ARCI), Centre for Laser Processing, Hyderabad, India*
[d]*Department of Nuclear Physics, University of Madras, Guindy Campus, Chennai-600 025, India*

Abstract — This research work deals with studies on the laser surface melting (LSM) of SUS 420F plastic mould steel and EN32B plain low carbon steel by a high power diode laser (HPDL). The laser treated samples were investigated by scanning electron microscopy (SEM) for microstructure and corrosion resistance was carried out using electrochemical method. In plastic mould steel, the microstructure is columnar dendrite and fine martensite microstructures with residual austenite phases are formed. The microstructures were transformed from columnar dendrite to randomly oriented ones, as the laser power was increased from 2 to 3 kW. On the other hand, the low carbon steel laser surface melted by the HPDL has created lath martensite microstructure. The potentiodynamic electrochemical corrosion method reveals improved corrosion resistance in the laser treated layers.

Keywords : *HPDL treatment, martensite, lath martensite, corrosion resistance.*

INTRODUCTION

The principle aim of the application of laser melting technique in the material surface processing is to improve the properties like corrosion resistance, wear resistance etc. Hence in this work, two steel materials i.e., SUS 420F and EN32B which have a multitude of application are considered for laser treatment by a high power diode

*Author for correspondence. E-mail : drmaha@annauniv.edu

laser (HPDL). SUS 420F steel is extensively used in the manufacturing of turbine blades, valve parts and plastic moulds [1]. This steel contains small amount of retained austenite and martensite structures [2]. Martensitic stainless steels are generally used for manufacturing components because they possess good mechanical properties and moderate corrosion resistance. Although the martensitic steel SUS 420F is the most popular material for various applications, the plain low carbon (EN32B) steel is also used in various mechanical components like gears, shaft, etc., [3].

At present scenario, laser processing technology is regarded as an advanced, highly efficient method, which has diverse fields of applications such as aerospace, automobiles, mechanical industries, etc,. Since it usually employs high laser output power density (10^3–10^6 W/cm^2) for heating the specimen and extreme rate of self quenching (10^3–10^6 °C/s), is obtained, the heat transfer and phase transformation processes are regarded as complex thermo-physical processes [4]. Laser hardening is a directed energy beam surface engineering technique that allows controlled heating followed by self quenching of steel compounds, leading to martensitic transformation upto a limited depth without affecting the bulk material [5]. Laser surface treatment using high power CO_2 and Nd : YAG lasers are employed as a reliable means of improving surface properties of tool steels [6].

In this study, high power diode laser (HPDL) surface melting technique is used to modify surface properties of SUS 420F steel and EN32B steel and their microstructure and phase transformation behaviors are analyzed. Corrosion test results of HPDL treated SUS 420F steel and EN32B steel are also presented.

Experimental Procedure :

The laser surface melting of SUS 420F plastic mould steel and EN32B steel was performed using a fiber coupled high power diode laser (LDF 6000) with a rectangular laser beam (17 mm × 2 mm) at an operating wavelength of 980 nm. The steel sample surface was irradiated with laser powers of 2.0, 2.5 and 3.0 kW at scanning speeds of 12 and 20 mm/s. After laser treatment, the laser treated track lengths were sectioned, metallographically polished and SUS 420F steel was etched using Vilella's reagent (picric acid 1 g, hydrochloric acid 5 ml and ethanol 100 ml) and EN32B steel was etched using NITAL 4% for microstructural analysis using scanning electron microscopy (HITACHI S-4700). The corrosion test was carried out with the samples of 5% NaCl solution at room temperature. The potentiodynamic electrochemical corrosion behaviors of the laser treated and untreated samples were evaluated under potentiostatic mode by using electrochemical workstation (CHI 7081).

RESULTS AND DISCUSSION

Microstructures :

SUS 420F steel — Microstructure analysis using High magnification Scanning Electron Microscopy confirmed the presence of martensite and various carbide phases formed at the hardened region. A small amount of retained austenite may also be present. Fig. 1(a-d) shows HRSEM images of the SUS 420F steel hardened at a laser power of 2.0 to 3.0 kW at a scanning speed of 12 mm/s. Base microstructure in Fig. 1(a) shows the presence of chromium carbides along the prior austenitic grain boundaries. The prior austenitic grain size is found to vary between 10–20 μm. The carbides are of sub micron (< 1 μm) size. The presence of columnar dendrite structures with the carbide network along the inter dendrite boundary, shown in Fig. 1(b) indicates the occurrence of dissolution and precipitation of the carbides. The presence of fine martensite needles within the dendrite could also be seen. Both the dendrite and martensite appear to have a preferential orientation as shown in Fig. 1(b). The macro level vertical orientation of dendrite and the micro level vertical and horizontal cross weave of martensite could be attributed to the sudden heating and cooling in a direction perpendicular to the surface of the specimen. Dendrite formation is generally associated with fast heating and cooling rates. The needle-like coarse martensite structures and aligned columnar dendrites are seen in the near-surface region of the laser treated sample as shown in Fig. 1(c). The laser treated zone consists predominantly of dendrite with fine martensite structure. The notable changes in the microstructure are widening of dendrite width as shown in Fig. 1(d). These changes indicate that as the power was increased from 2 to 3 kW for a scanning speed of 12 mm/s, both the cooling rate and the temperature gradient could have been reduced. Whenever the temperature gradient decreases the morphology of the dendrite transforms from columnar dendrite to equiaxed dendritic and as and when the cooling rate gets decreased, the morphology of the microstructure features tends to become coarser. Khan et al. [7] have observed similar changes in the morphology of the dendrite in their investigation on laser beam welding of martensitic stainless steel AISI 416 and AISI 440. Stephen Skvarenina and Yung C. Shin [8] have reported that the laser treated zone consists of needle shaped martensite. In our study, the laser treated zone consists of fine martensite needles within the dendrite microstructures.

EN32B steel — Fig. (2) shows the microstructure of the untreated and laser treated regions of EN32B alloy steel. The microstructure of the as received steel shows the presence of pro eutectoid ferrite and pearlite (Fig. 2a). The size of the pro eutectoid ferrite is found to vary between 20–40 μm. The pearlite colonies are found to exhibit different morphologies such as triangular, trapezoidal with different aspect ratios. On

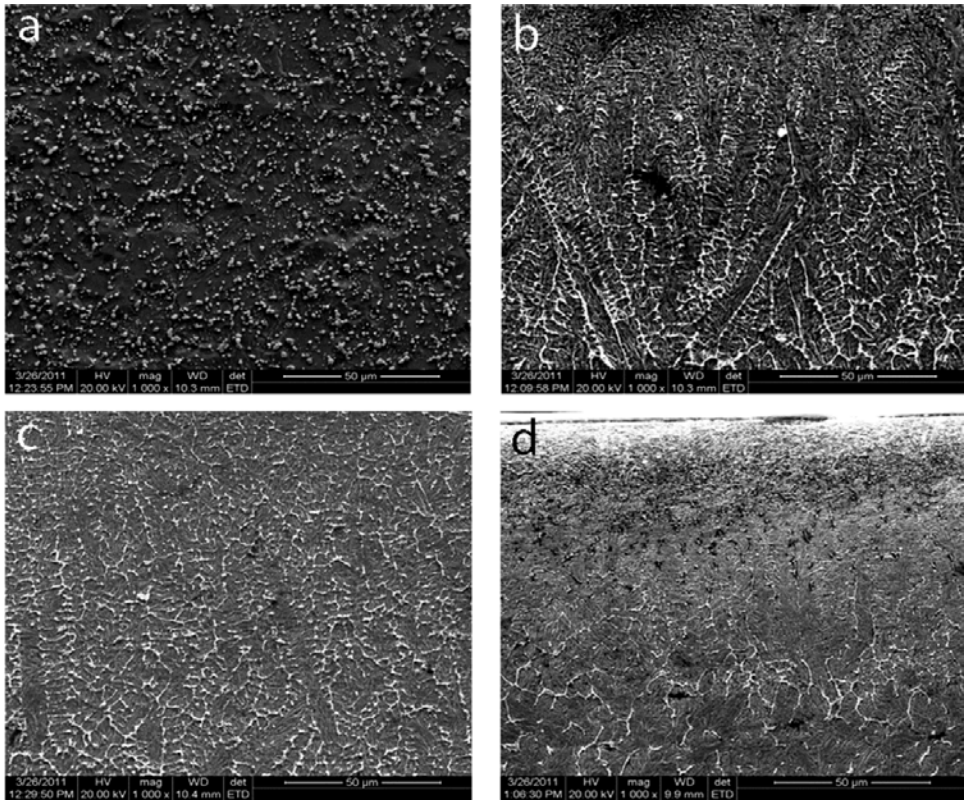

Fig. 1. HRSEM images of laser-treated SUS 420F steel at various laser powers with constant scanning speed of 12 mm/sec : (a) unaffected substrate (1000×), (b) for laser power of 2.0 kW (1000×), (c) for laser power of 2.5 kW (1000×) (d) for laser power of 3.0 kW (1000×).

an average, the colony sizes range between 10–50 μm. The laser treated (2.0 kW) top surface layer shows the presence of packets of lath martensite and bainite (Fig. 2b). Within each packet the martensite laths are oriented in one particular direction. The size of the packets range between 5–20 μm, and the presence of only the lath martensite on the top surface layer is indicated. The microstructure of EN32B samples treated with laser beam of 2.5 kW at a scan speed of 12 mm/sec is shown in (Fig. 2c). The laser treated layer reveals the presence of packet of martensite with evenly oriented broad laths (Fig. 2c). On laser treatment with 3 kW power at scanning speed of 12 mm/sec, the top surface exhibited the presence of packets of lath martensite (Fig. 2d). The irradiation of laser on the specimen surface results in a rapid heating of surface layer to the austenization temperature range. Subsequent moderate cooling

rate due to the self quenching led to the formation of lath martensite and bainite with ferrite structures (Fig. 2d). The laser treatments of the samples in heating and cooling rate were responsible for the microstructural differences between the laser treated zones. The rapid cooling rate of the laser treated material results in a fine microstructure. Laser treatment of the materials, induces a thermal cycle to the material which is far from equilibrium due to the rapid heating and cooling rates [9]. It has been found that non-equilibrium heating of steels leads to an increase in the critical temperatures even more than 250°C [10].

Electrochemical corrosion test :

SUS 420F steel — Fig. (3) shows the potentiodynamic polarization curves of the untreated and laser treated SUS 420F steel specimens in 5 wt % NaCl solutions at

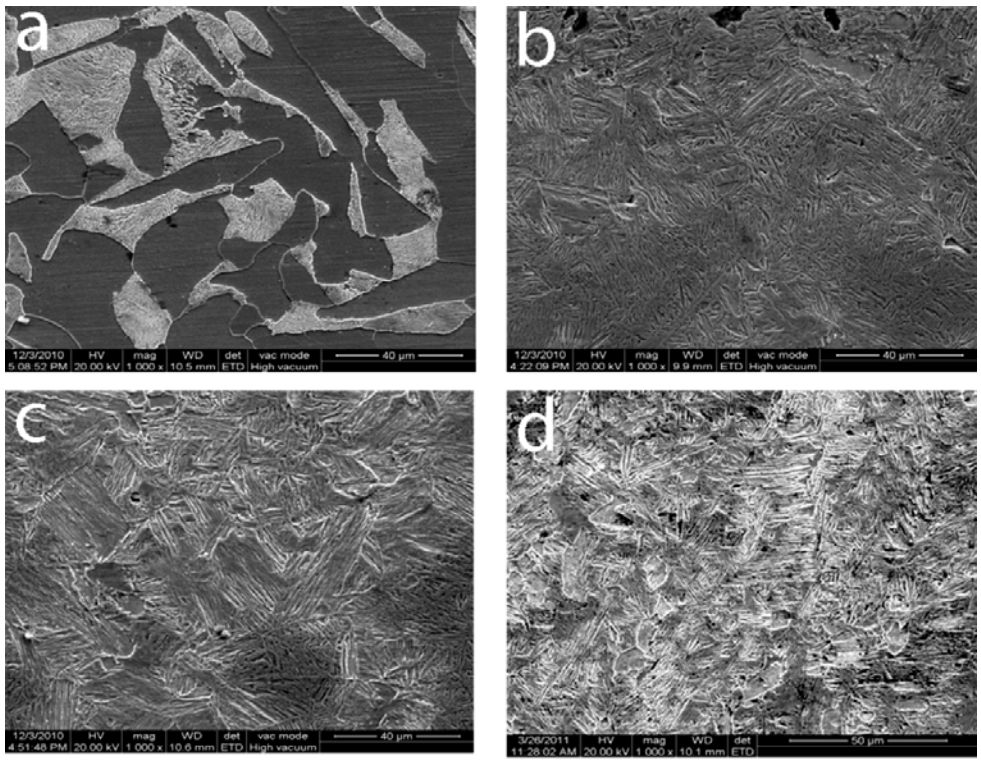

Fig. 2. HRSEM images of laser-treated EN32B steel at various laser powers with constant scanning speed of 12 mm/sec : (a) unaffected substrate (1000×), (b) for laser power of 2.0 kW (1000×), (c) for laser power of 2.5 kW (1000×) (d) for laser power of 3.0 kW (1000×).

25°C. It was observed that the corrosion potential shifted towards the noble direction on increasing the laser power compared to untreated steel. However, no constant current density can be observed in Fig. 3 and active to passive transition may be observed above 0 V [11]. It can be seen from Fig. 3 that the untreated specimens show predominant current oscillations. This fluctuation may be due to the unstable oxide layer in the corrosive media of 5 wt% NaCl solutions. The resistance to corrosion of the laser hardened increases with increasing the laser power. For 3.0 kW laser treated specimens, the pitting corrosion does not occur and the passive film formed has good stability until the end of the growth potential in the 5 wt% NaCl medium. The passivation elements on the SUS 420F steel such as Cr and Mo are not much enough to form stable passive film on the surface [12]. Mahmoudi et al [13] have reported that during the laser hardening, the passivation element Cr dissolve to carbide form of CrC, which leads to a considerable decrement in the Cr content of the alloy which reduced the corrosion resistance. In our case up to 3.0 kW laser power hardening processes there is no significant change in the Cr content which

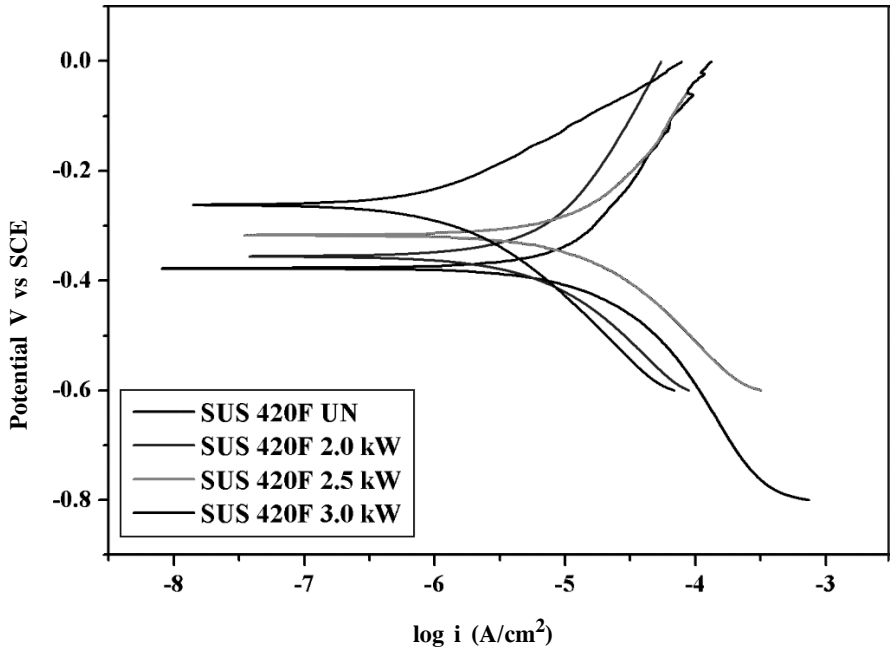

Fig. 3. Potentiodynamic polarization curves of untreated and laser treated SUS 420F steel specimens in 5% NaCl at 25 °C; (a) untreated specimen; (b) laser-treated specimen at 2.0 kW; (c) laser-treated specimen at 2.5 kW; (d) laser-treated specimen at 3.0 kW.

results in the increasing corrosion resistance. The Cl^- ions have greater affinity to penetrate into the oxide layer due to chemical alteration during the pitting nucleation in such a way that the dissolution of SUS 420F steel becomes difficult compared to untreated specimens.

Conde et al. [14] have reported the corrosion behavior of AISI 420 and AISI 430 stainless steels with respect to different laser scanning speeds. They have observed that for lower and higher scanning speeds there is no improvement in corrosion resistance and for intermediate scanning speed it decreases. They have suggested that the duplex austenite structure appeared for intermediate rates have a deleterious effect on the corrosion resistance. However, in our study we have observed that the corrosion resistance gradually increases as laser power increases due the increase in hardness and change in microstructures.

Kwok et al. [15] have reported erosion and pitting corrosion behavior of laser surface melted UNS S4200 stainless steel. They have observed a corrosion potential of –476 and –361mV for the sample surface melted by 1.1 and 1.7 kW laser power respectively. Also they observed pitting corrosion potential on the laser surface melted alloys. Interestingly we have not observed any pitting corrosion in the potentiodynamic polarization curve. This may be due to the uniform hardening on the surface by high power laser treatment. Otherwise, the high power laser treatment on SUS 420F steel surface did not melt even at high scanning speeds. This results in the decreasing of corrosion potential of 3.0 kW laser power treated sample at 20 mm/s scanning speed. In the previous case, they observed a high corrosion potential for the laser power of 1.7 kW at 15 mm/s and 25 mm/s scanning speed, when compared to lower laser power treated samples which indicate the surface melting process. In our case, the corrosion potential of SUS 420F steel has increased gradually with respect to the laser power. This may be attributed to the formation of dendrite and carbide structures on the laser hardened surface.

In the potential range between –0.15V to –0.05V, a current plateau was observed which indicates thickening of the surface oxide layer. The curve had significant shift towards the positive direction with decreased current density throughout the potential range. This behavior can be attributed to the stable layer over the laser treated surface of the specimen. The potential curves shown in Fig. 3, show high corrosion potential for laser treated samples and the corrosion rate have decreased. This increase in corrosion potential is due to the interaction of Cl^- ions with the surface of the SUS 420F specimens. Thus, on laser treatment the surface morphology, after carrying out electrochemical assays, has clearly showed that on increasing the laser power, a lower corrosion rate can be achieved.

EN32B steel — The electrochemical corrosion behavior of En32B steel, treated with various laser powers at constant scanning speed of 12 mm/sec were studied using polarization experiments. The corrosion potential, corrosion current density and corrosion rate are determined through the extrapolation of Tafel plots, which are shown in Fig. 5. The laser treated samples passivate in the corrosion potential ranging between –455 to –447 mV. The higher corrosion resistance for the laser treated samples is due to the reduction in corrosion current density, which is found to be in the sites for potential nucleation. It was also noted that passivation was more pronounced in the laser treated samples [16]. Khalfallah et al. [17] have reported that the surface melting improves the corrosion resistance. In the present study, the corrosion resistance is improved for the laser surface treated layer as compared to the untreated sample. The better corrosion resistance obtained in the laser treated sample at medium laser power (2.5 kW), is due to the high hardness and absence of ferrite microstructure. Abdolahi et al. [18] have observed that the laser surface alloying sample shows a five-fold increase in the corrosion resistance compared to untreated low carbon steel. In the present study, an increase in the corrosion resistance

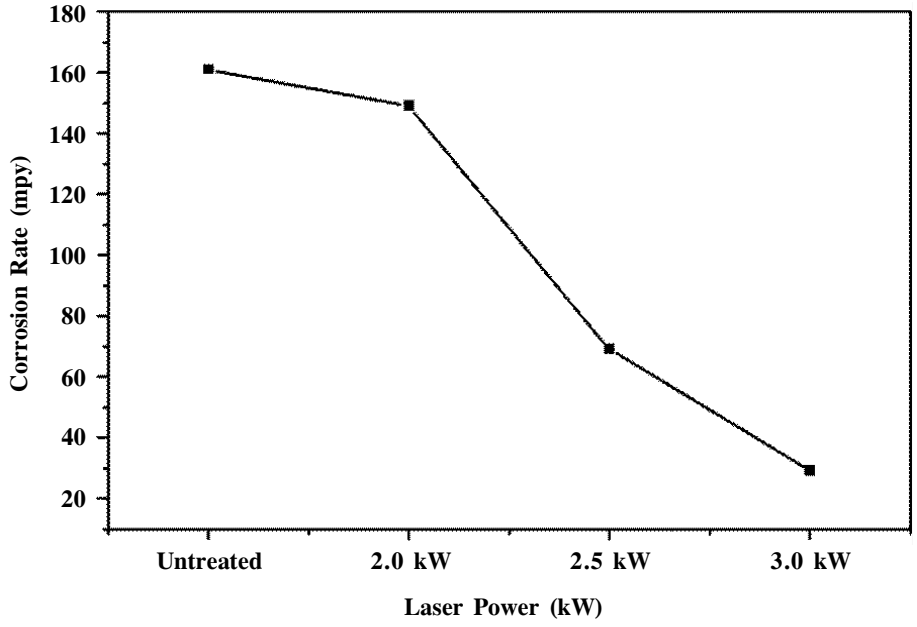

Fig. 4. Electrochemical test : corrosion rate curves of untreated and laser treated for SUS 420F steel.

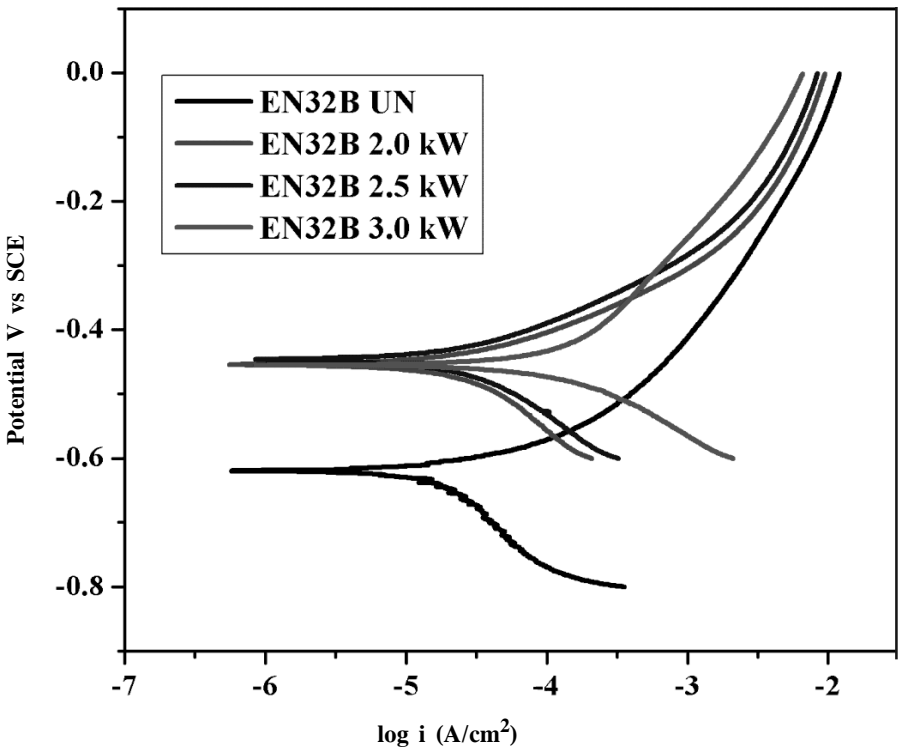

Fig. 5. Potentiodynamic polarization curves of untreated and laser treated EN32B low carbon steel specimen in 5% NaCl at 25 °C; (a) Untreated specimen; (b) laser-treated specimen at 2.0 kW; (c) laser-treated specimen at 2.5 kW; (d) laser-treated specimen 3.0 kW.

of 2 to 2.5 times can be observed for laser treated samples compared to untreated sample.

The microstructure of the laser treated samples of SUS 420F steel exhibits dendrite and martensite structures while for the laser treated EN32B steel it contains lath martensite and bainite structures. The corrosion resistance increases very much after laser surface treatment for SUS 420F steel due the formation of dendrite and martensite structures. On the other hand, the EN32B it is comparatively less due the formation of lath martensite and bainite structures. In addition to this, homogenization of microstructure also contributes to improvement in the corrosion properties. The overall improvement of corrosion resistance of a SUS 420F laser treated layer is more than that of laser treated EN32B steel. This is attributed due the formation of dendrite with martensite and also high chromium medium carbon content of SUS 420F steel.

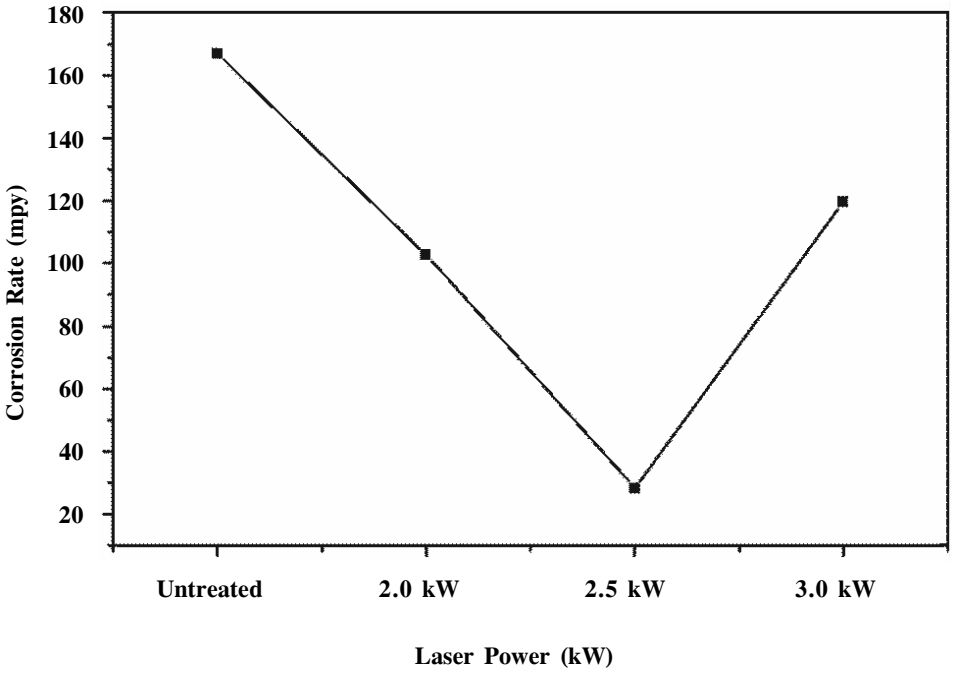

Fig. 6. Electrochemical test : corrosion rate curves of untreated and laser treated for EN32B low carbon steel

CONCLUSION

In this research work laser surface treatment of SUS 420F and EN32B steel materials were carried out and their microstructural and corrosion behavior were analyzed. It was found that the laser treatment has refined the carbide precipitates homogeneously in the ferrite parent matrix. In the SUS 420F steel, the laser treated layer consists of columnar dendrite and fine martensite microstructures with residual austenite phases are also formed. The EN32B untreated sample consists of pro eutectoid ferrite and pearlite. The laser treated area consists of packets of lath martensite and bainite structures. The inference from this study suggests that high power laser treatment is an effective method to treat metal surfaces to improve corrosion resistance of SUS 420F steel and EN32B steel. Thus laser treated specimens could be considered as potential candidates for plastic injection mould and machine component applications.

REFERENCE

1. A. F. Candelaria and C. E. Pinedo, *J. Mater. Sci. let.*, 22, 1151, (2003).
2. Bulent Kurt, Nuri Orhan, Ilyas Somunkiran and Mehmet Kaya, *Mater. Des.*, 20, 661, (2009).
3. M. Stanford, P. M. Lister, C. Morgan and K. A. Kibble., *J. Mater. Proce. Tech.*, 209, 961, (2009).
4. Khansaa Dawood Salman, *Eng. Tech. J.*, 27, 6, 1151, (2009).
5. A. Basu, J. Chakraverthy, S. M. Shariff, G. Padmanabham, S. V. Joshi, G. Sundararajan, J. Dutta Majumdar and I. Manna, *Scrip. Material.*, 56, 887, (2007).
6. Ghazanfar Abbas, Lin Li, Uzma Ghazanfar and Zhu Liu, *Wear.*, 260, 175, (2006).
7. M. M. A. Khan, L. Romoli, R. Ishak, M. Fiaschi, G. Dini and M. De Sanctis, *Opt. Laser. Techn.*, 44, 1611, (2012).
8. Stephen Skvarenina and Yung C-Shin, *Surf. Coat. Techn.*, 201, 2256, (2006).
9. J. R. Bradley and S. Kim, *Metall. Trans. A.*, 19, 8, 2013, (1988).
10. A. Jacot and M. Rappaz, *Acta Material.*, 45, 2, 575, (1997).
11. D. I. Pantelis, E. Bouyiouri, N. Kouloumbi, P. Vassiliou and A. Koutsomichalis, *Surf. Coat. Techn.*, 298, 125, (2002).
12. C. T. Kwok, F. T. Cheng and H. C. Man, *Surf. Coat. Techn.*, 202, 336, (2007).
13. B. Mahmoudi, M. J. Torkamany, A. R. Sabour Roug Aghdam and J. Sabbaghzade, *Mater. Des.*, 31, 2553, (2010).
14. A. Conde, R. Colaco R. Vilar and J. de. Damborenea, *Mater. Des.*, 21, 441, (2000).
15. C. T. Kwok, H. C. Man and F. T. Cheng, *Surf. Coat. Techn.*, 126, 238, (2000).
16. J. Hu, P. L. Wu, L. C. Kong and G. Liu, *Mater. Lett.*, 61, 5181, (2007).
17. I. Y. Khalfallah, M. N. Rahoma, J. H. Abboud and K. Y. Benyounis, *Opt. laser. Tech.*, 43, 806, (2011).
18. B. Abdolahi, H. R. Shahverdi and M. J. Torkamany, *Appl. Surf. Sci.*, 257, 9921, (2011).